sciendo

POLISH MARITIME RESEARCH 1 (105) 2020 Vol. 27; pp. 18-28
10.2478/pomr-2020-0002

RESEARCH ON SHIP HULL OPTIMISATION OF HIGH-SPEED SHIP BASED ON VISCOUS FLOW/POTENTIAL FLOW THEORY

Zhang Baoji
Shanghai Maritime University, China

ABSTRACT

In order to quickly obtain practical ship forms with good resistance performance, based on the linear wave-making resistance theory, the optimal design method of ship forms with minimum total resistance is discussed by using the non-linear programming (NLP) method. Taking the total resistance as the objective function (the Michell integral is used to calculate the wave-making resistance and the equivalent plate friction resistance formula is used to calculate the frictional resistance), the hull surface offset as the design variable and appropriate displacement as the basic constraints, and considering the additional constraints, the hull bow shape and the whole ship are optimised, and an improved hull form is obtained. The resistance of the ship before and after optimisation is calculated by the CFD method to further evaluate the resistance reduction effect and performance after optimisation. Finally, an example of optimisation calculation of an actual high-speed ship is given. The obvious resistance reduction results confirm the reliability of the optimisation design method.

Keywords: potential flow theory; CFD; high speed ship; ship form optimisation

INTRODUCTION

Under the concept of "green ship" design and construction, it is urgent to build a resource-saving and environmentally optimised shipbuilding industry. The international rules and regulations that will soon come into force require future ship design to be safer, more environmentally friendly and more economical. Therefore, energy saving and emission reduction have become the theme of foreign ship design. The key to reducing fuel consumption and carbon emissions is to reduce the actual navigational resistance of ships under design conditions, that is, to design a "green ship form" [1]. In the past, ship form design strongly relied on the experience of ship model series tests and designers, and lacked a scientific evaluation system. In recent years, with the continuous progress of mathematical knowledge and the rapid development of computer technology, numerical evaluation technology, optimisation theory and hull geometry reconstruction technology are being effectively integrated. Under given constraints, it is possible to seek the optimal design of a ship form with optimal navigational performance, which greatly promotes advances in ship form design from the traditional empirical mode to an intelligent and knowledge-based mode [5]. Based on potential flow theory, Japanese scholars began to study ship form optimisation as early as the 1960s. The main representative is Kazuo Suzuki (Kazuo, 2001), who used the wave-making resistance calculated by the Rankine source method and combined this with the sequential quadratic programming(SQP) method to study the ship form optimisation problem with minimum wave-making resistance. In addition, C. C. Hsiung (Hsiung, 1981&1984) of Canada first proposed the method of expressing the hull surface with a 'tent function'. The Michell integral method was used to calculate the wave-making resistance, which was expressed as a function of its shape value, thus constituting a quadratic programming problem for ship form optimisation. In China,

Ye Heng-Kui (Ye, 1985) first discussed the optimisation of the ship form with minimum wave-making resistance based on linear wave-making theory. The Michell integral method was used to calculate the wave-making resistance, C.C. Hsiung's tent function was used to express the hull surface, and the mixed penalty function method was used to transform the constrained optimisation problem into an unconstrained optimisation problem. Ma Kun (Ma, 1994) conducted a lot of research on the optimisation of the minimum resistance ship form based on the theory of wave-making resistance, and studied methods of ship form design with both minimum wave-making resistance and minimum total resistance. The control of viscous separation at the stern is taken as the constraint condition, and the minimum total resistance of the hull is taken as the objective function. This method not only simplifies the calculation model and improves the computation speed, but also considers the influence of tail viscosity. Most of the above studies are based on the NLP method. Generally speaking, this kind of ship form optimisation process will often result in strange shapes that lack practical significance, but it is easy to understand the influence of the change of hull shape on the resistance performance from the mechanism. This is of great significance for clarifying the optimisation direction and guiding the design modification. In order to obtain a practical ship type, we can add the corresponding restriction conditions in the refinement process according to experience to make the optimised ship type closer to a practical ship type, and carry out the optimisation calculation again.

In order to obtain the ship type with the best sailing performance, researchers have begun to establish the relationship between ship navigation performance and ship type parameters according to a regression formula for series of ship model test results, and to carry out ship type optimisation design at the design stage. Wang Bin (Wang, 2013) proposed a multi-objective ship type optimisation system that minimises the wave resistance and the increasing wave resistance, calculated the wave-making resistance using CFD software, and calculated the wave resistance based on the potential flow theory. The full parameterised model is established in FriendShip software, and the above modules are integrated through a self-programming interface. The feasibility of this method for the optimisation of wave-resistant ships is verified by an example of an oil tanker. Zhang Wen-Xu (Zhang, 2012) studied the multi-disciplinary optimisation of shipboard vessels in the waves of container ships based on an Energy Efficiency Design Index (EEDI). This takes the navigation performance (wave resistance, EEDI energy efficiency index) as the objective function in the wave and the full parametric model based on the ship's wave-resistance standard, and uses the ISIGHT multidisciplinary optimisation platform to carry out integrated integration, which can be used in different optimisation strategies to complete the waves in the ship type optimisation. Based on OPTShip-SJTU, a self-developed ship form optimisation platform, Wu Jian-Wei and Liu Xiao-Yi et al. (Wu, 2016; Liu, 2016) studied the ship form optimisation problem based on hydrodynamic performance. Based on linear wave resistance theory, the FFD method was used as the hull geometry reconstruction method, and a multi-objective genetic algorithm was used to optimise the resistance performance and seakeeping performance of the hull. Huang Fu-Xin et al. (Huang, 2015) proposed a proxy model based on the radial basis function (RBF) to approximate the objective function, to optimise the resistance performance and improve the seakeeping performance of ships. The objective function was evaluated by linear wave-making resistance theory and slender theory. Zou Yong (Zou, 2012) studied the high performance ship optimisation design method based on the Energy Efficiency Design Index (EEDI). Taking the two important factors influencing the ship's EEDI as speed and load capacity, a multi-objective genetic algorithm was used to optimise the model. The results show that the energy efficiency level of the ship can be effectively improved in the early stage of high-performance ship design. Most of the above studies take the wave resistance and EEDI as the objective function, which are implemented in a business optimisation platform and self- programming interface. At present, although CFD-based ship form optimisation has become possible, it takes a long time to evaluate the resistance of a ship by the CFD method. If combined with the optimisation method, it is difficult to achieve without a supercomputer or large workstation, especially for some early ship form designers. Therefore, in the preliminary optimisation design stage of a ship, it is more appropriate to use the potential flow theory, which has a fast evaluation ability and a certain engineering accuracy. Moreover, as an example, an offshore wind power operation and maintenance vessel has very high speed, and its main resistance component is the wave-making resistance. Therefore, in the optimisation design, the main consideration is how to reduce the wave-making resistance. Finally, the CFD method is more appropriate to evaluate the final drag reduction effect. Therefore, for the purpose of minimising the total resistance of a full-scale ship, an optimal design method is proposed based on the Michell integral method and the NLP method. The hull shape is optimised with total resistance as the objective function, with the hull surface offset as design variables, with an appropriate displacement as a constraint, and with the allowable variation of the hull shape as an additional constraint. To evaluate more precisely the resistance reduction effect of the full-scale ship by the present method, the wave-making resistance is re-calculated with the CFD method for both the optimised ship and the original one. Finally, numerical optimisation examples for full-scale container ships are provided, and indicate that the resistance is reduced distinctly by this optimal design method.

POTENTIAL FLOW THEORY

MICHELL INTEGRAL FORMULA

Letting a uniform flow be the basic flow, the volatility potential superimposed on this basic flow satisfies the linear free surface condition. Under the conditions of a thin hull,

infinite water depth and symmetrical flow, Michell uses the method of separation of variables to get the corresponding velocity potential and the corresponding wave-making resistance formula [4].

Take the right-hand rectangular coordinate system fixed on the hull: the origin o is taken on the undisturbed stationary surface and is at the bow of the load waterline where the ox axis and the oy axis coincide with the still water surface. The ship is in uniform linear motion along the X-axis in a negative direction at a speed of U. According to the principle of motion conversion, it can be considered that the ship is in a uniform flow of velocity U, as shown in Fig. 1.

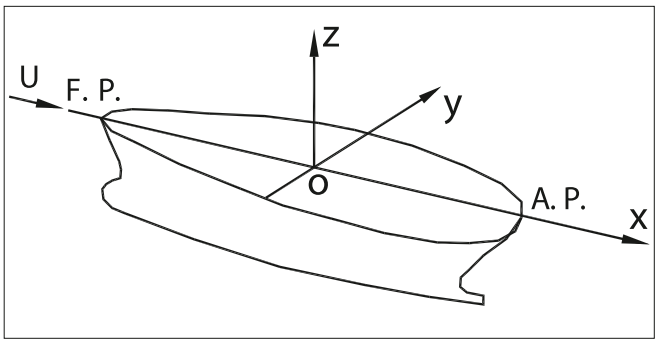

Fig. 1. Coordinate system

$$R_w = \frac{4\rho g K_0}{\pi} \int_0^{\pi/2} (I^2 + J^2) \sec^3 \theta d\theta \tag{1}$$

where

$$I + iJ = \int_{-T}^{0} dz \int_{-L/2}^{L/2} f_x(x, z) e^{K_0 z \sec^2\theta + iK_0 x \sec\theta} dx$$

$$I = \int_{-d}^{0} e^{K_0 z \sec^2\theta} dz \int_{-L/2}^{L/2} f_x(x, z) \cos(K_0 x \sec\theta) dx$$

$$J = \int_{-d}^{0} e^{K_0 z \sec^2\theta} dz \int_{-L/2}^{L/2} f_x(x, z) \sin(K_0 x \sec\theta) dx$$

where K_0 is the wave number, and $K_0 = g/c^2$, c is the ship speed; g is the gravitational acceleration; ρ is the water density; $y = \pm f(x, z)$ is the surface equation of the ship form; L is the length, d is the draft.

TENT FUNCTION

The key to the numerical calculation of wave resistance using Michell's integral method is how to express the hull function [2]. However, the hull surface is usually expressed in the form of discrete point values, whereas the tent function can relate hull shape values to the formula of wave-making resistance. When using the tent function to express the hull value, the hull surface is first divided into rectangular grids with a certain number of waterlines and station numbers, as shown in Fig. 2.

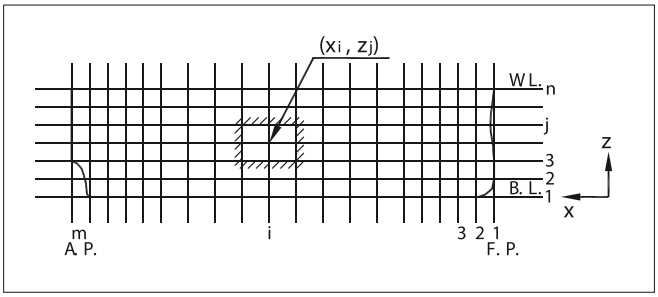

Fig. 2. Hull grid arrangement

When deploying the station number and waterline, place the first station line at the forefront of the hull and the last station line at the rear end of the hull, with the first waterline being the baseline and the last waterline being the design waterline. The rectangular cells at (x_i, z_i) grid points are composed of (i-1), (i+1) station number lines and the (j-1), (j+1) the waterlines. Now define a unit tent function, as shown in Fig. 3, which has a value equal to 1 at the grid point (x_i, z_i) and a value equal to 0 at the cell boundary.

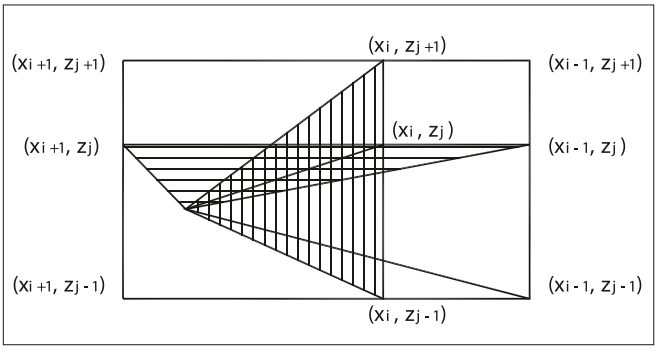

Fig. 3. Unit tent function

The unit tent function $h^{(i,j)}(x, z)$ related to the grid point (x_i, z_i) can be written as follows:

$$h^{(i,j)}(x,z) = \begin{cases} (1-\frac{x_i - x}{x_i - x_{i-1}}) \cdot (1-\frac{z_j - z}{z_j - z_{j-1}}) & x_{i-1} < x < x_i, z_{j-1} < z < z_j \\ (1-\frac{x_i - x}{x_i - x_{i-1}}) \cdot (1-\frac{z_j - z}{z_j - z_{j+1}}) & x_{i-1} < x < x_i, z_j < z < z_{j+1} \\ (1-\frac{x_i - x}{x_i - x_{i+1}}) \cdot (1-\frac{z_j - z}{z_j - z_{j-1}}) & x_i < x < x_{i+1}, z_{j-1} < z < z_j \\ (1-\frac{x_i - x}{x_i - x_{i+1}}) \cdot (1-\frac{z_j - z}{z_j - z_{j+1}}) & x_i < x < x_{i+1}, z_j < z < z_{j+1} \\ 0 & other \end{cases} \tag{2}$$

Looking closely at the expression, although the unit tent function $h^{(i,j)}(x, z)$ is not a linear function, in each quadrant of a cell, $h^{(i,j)}(x, z)$ is a linear function of x for a fixed z, or for a fixed x, $h^{(i,j)}(x, z)$ is a linear function of z. According to this feature of the tent function, the tent function family can be used to form a function together with the hull value to approximate the hull surface. If the hull value at (x_i, z_i) is y_{ij}, the approximate hull function can be defined as:

$$h(x, z) = \sum_i \sum_j y_{ij} h^{(i,j)}(x, z) \quad (3)$$

According to the tent function, we can see that at the grid point (x_i, z_i), $h^{(i,j)}(x, z) = 1$, so

$$h(x, z) = y_{ij} \quad (4)$$

Or

$$h(x, z) = h^{(i,j)}(x, z)$$

Eq. (4) can be used to approximate the surface function of the hull. The degree of approximation is related to the size of the mesh.

CFD BASIC THEORY

CONTROL EQUATION

The whole flow field uses the continuity equation and RANS equations as the governing equations [17]:

$$\frac{\partial U_i}{\partial x_i} = 0 \quad (5)$$

$$\rho \frac{\partial U_i}{\partial t} + \rho U_j \frac{\partial U_i}{\partial x_j} = -\frac{\partial \hat{p}}{\partial x_i} + \frac{\partial}{\partial x_j}\left(\mu \frac{\partial U_i}{\partial x_j} - \overline{\rho u_i u_j}\right) f_i^* \quad (6)$$

where $U_i=(U, V, W)$ is the velocity component in the $x_i=(x, y, z)$ direction, and $\hat{p}$, μ, $-\overline{\rho u_i u_j}$ and f^*_i are the fluid density, static pressure, fluid viscosity, Reynolds stresses and body forces per unit volume, respectively.

TURBULENCE MODEL

The turbulence model adopts the RNG k-ε model, and the forms of the turbulence energy transport equation and energy dissipation transport equation are as follows [10]:

$$\rho \frac{dk}{dt} = \frac{\partial}{\partial x_i}\left[(\alpha_k \mu_{eff}) \frac{\partial k}{\partial x_i}\right] + G_k + G_b - \rho\varepsilon - Y_M \quad (7)$$

$$\rho \frac{d\varepsilon}{dt} = \frac{\partial}{\partial x_i}\left[(\alpha_\varepsilon \mu_{eff}) \frac{\partial \varepsilon}{\partial x_i}\right] + C_{1\varepsilon}\frac{\varepsilon}{k}(G_k + C_{3\varepsilon} G_b) - C_{2\varepsilon}\rho\frac{\varepsilon^2}{k} \quad (8)$$

where μ_{eff} is the effective dynamic viscosity, k and ε are the turbulent kinetic energy and the turbulent dissipation rate. The quantities ∂_k and ∂_ε are the inverse effective Prandtl numbers for k and ε, respectively; G_k is the generation of turbulent kinetic energy by the mean velocity gradients; G_b is the generation of turbulent kinetic energy by buoyancy; Y_M represents the contribution of the fluctuating dilatation in compressible turbulence; $C_{1\varepsilon}$, $C_{2\varepsilon}$, and $C_{3\varepsilon}$ are empirical constants.

VOF METHOD

The volume of fluid (VOF) method is used to capture the free surface. It is a surface tracking method fixed under the Euler grid and simulates the multiphase flow model by solving the momentum equation and the volume fraction of one or more fluids. Within each control volume, the sum of the volume fractions of all the phases is one. As to Phase q, its equation is [18]:

$$\frac{\partial \alpha_q}{\partial t} + \frac{\partial (u\alpha_q)}{\partial x} + \frac{\partial (v\alpha_q)}{\partial y} + \frac{\partial (w\alpha_q)}{\partial z} = 0 \quad (9)$$

where $q = 0$ means that the unit is filled with water, $q = 1$ means that the unit is filled with air, a_0 and a_1 are respectively the volume fractions of air and water, and is the interface of water and air.

DISCRETISATION AND SOLUTION OF EQUATIONS

The commonly used numerical methods include the finite volume method, finite element method and finite difference method [19]. The finite volume method is the intermediate product of the finite element method and finite difference method. It is also one of the most widely used discrete methods in the field of CFD. In this paper, the finite volume method is used to discretise the governing equations.

A general form of governing equations for one-dimensional steady convection diffusion problems is

$$\frac{d(\rho(\rho u))}{dx} = \frac{d}{dx}\left(\Gamma \frac{d\varphi}{dx}\right) \quad (10)$$

where φ is the generalised variables, which can be physical quantities to be sought for velocity and wave forces. Γ is the generalised diffusion coefficient corresponding to φ. S is the generalised source terms, in the passive case $S = 0$.

The central finite difference scheme is used to obtain the discrete equations.

$$\alpha_F \varphi_F = \alpha_W \varphi_W + \alpha_E \varphi_E \quad (11)$$

ESTABLISHMENT OF THE SHIP FORM OPTIMISATION MODEL

OBJECTIVE FUNCTION

In the present study, the total resistance R_T is selected as the objective function in the optimisation design process, R_T is expressed as the sum of wave resistance R_W and the frictional resistance of a flat plate R_F, namely

$$\text{Min } R_T = R_W + R_F \quad (12)$$

where the R_W is calculated by the Michell integral method [20].

$$R_F = \frac{1}{2}\rho U_\infty^2 S C_{f0} \tag{13}$$

C_{f0} is the frictional resistance coefficient of a flat plate:

$$C_{f0} = 0.463\ (\log_{10} Re)^{(-2.6)}$$
$$Re = \frac{UL}{\nu} \tag{14}$$

where Re is the Reynolds number based on the body length, ν is the viscosity coefficient of fluid motion, S is the wet surface area, which is the function of the hull coordinates. It is approximately calculated by the tent function.

DESIGN VARIABLES

The whole Wigley hull form and the bow of a high-speed ship are selected as the deformation area respectively. The design waterline and the bottom of the hull are fixed, as shown in Fig. 4.

CONSTRAINT CONDITIONS

The constraints are mainly considered to satisfy the geometric constraints and drainage volume requirements. There are two as follows:

1) All ship offsets are non-negative, namely: $y\ (i, j) \geq 0$;
2) Ensure the necessary displacement volume, namely: $V \geq V_0$ where V_0, V are the displacement volumes of the original hull and the improved hull, respectively.
3) Additional constraint: $H - |y_0(i, j) - y(i, j)| \geq 0$;

where $y_0(i,\ j)$ is the offsets of the original hull; $|y_0(i, j) - y(i, j)|$represents the deformation values of each point of the improved ship form relative to the original ship form. The H value is the control value of deformation, and it should be selected properly.

OPTIMISATION METHOD

The SUMT interior point method in nonlinear programming is adopted in the ship hull optimisation; that is, an additional term reflecting the influence of constraints is added to the objective function to form an unconstrained optimisation problem. Then, the gradient method in the direct search speed method is selected to find the minimum point and get the minimum resistance ship type. The general form of its mathematical model is as follows [8]:

Design variables: $X = [x_1, x_2, \ldots\ldots, x_n]^T$
Objective function: $\min f(X)$
Constraints condition: $g_i(X) \geq 0,\ i = 1, 2, \ldots\ldots, p.$
$h_i(X) \geq 0, j = 1, 2, \ldots\ldots, q.$
Constructing penalty function:

$$F(X, r^{(k)}, s^{(k)}) = f(X)\ r^{(k)} \sum_{i=1}^{p} \left\{ \frac{|g_i(X)| - g_i(X)}{2} \right\}^2 +$$
$$+ s^{(k)} \sum_{i=1}^{p} \{h_i(X)\}^2 \tag{15}$$

In the formula, $f(X)$ is the objective function of the original problem, $r^{(k)}$, $s^{(k)}$ is a variable parameter that is constantly adjusted with the increase of K in the optimisation process. It is called a penalty factor and K is the number of iterations. In the process of optimisation, a series of unconstrained optimisation calculations of penalty functions are carried out after a series of penalty factors $r^{(k)}$ and $s^{(k)}$ are determined. When $K \to \infty$, the advantage of the penalty function gradually approaches the best of the original objective function. Therefore, this method is often referred to as the "sequence unconstrained minimisation method", or SUMT method for short.

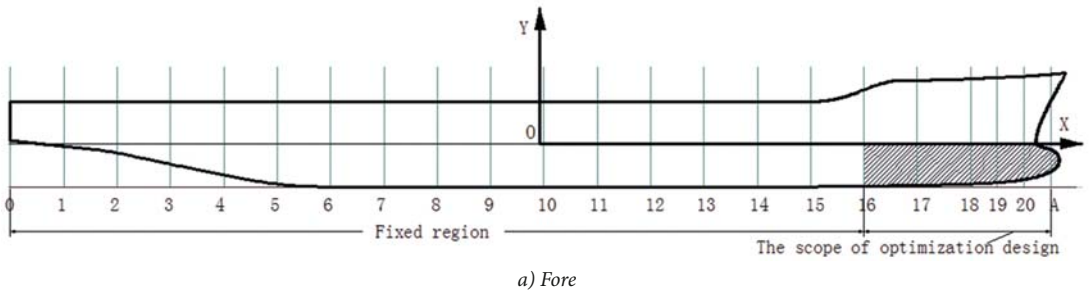

a) Fore

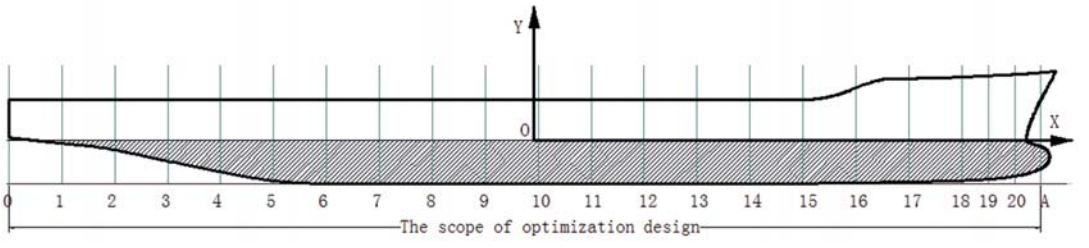

b) Whole ship

Fig. 4. The scope of the optimisation design

SHIP FORM OPTIMISATION PROCESS

The flow chart of ship form optimisation is shown in Fig. 5. First, the initial hull form value file is input, which includes the initial hull form elements and shape values, design scope, number of design variables, design speed, initial parameters of optimisation calculation, etc. Then, according to basic constraints 1) and 2), the optimisation calculation is carried out to get the improved ship form. The CFD method is used to further evaluate whether the total resistance of the improved ship is the smallest. If not, the designer can attach constraint condition 3), limit the deformation, then the optimisation calculation is carried out and the CFD method is used to evaluate the ship until the practical ship with the least resistance is obtained. In the objective function of the optimisation mathematical model, the Michell integral method, which can be used to calculate the wave resistance quickly, is used to facilitate the realisation of the optimisation calculation, but the calculation results and test values deviate greatly. The CFD method is used to evaluate the resistance of the ship before and after optimisation.

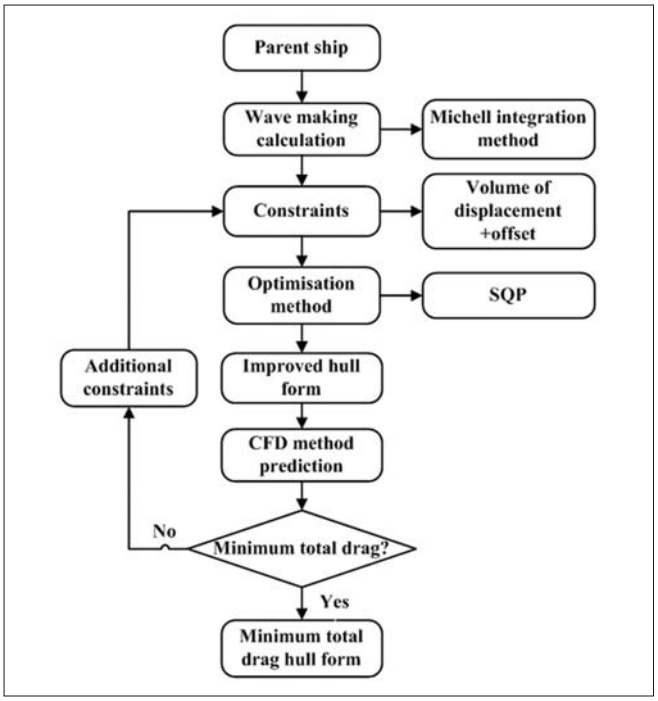

Fig. 5. Flow chart of ship form optimisation calculation

EXAMPLE OF SHIP OPTIMISATION FOR WIND POWER OPERATION AND MAINTENANCE SHIP

Taking a certain type of high-speed vessel as the research object, its main dimensions are shown in Table 1. The ship form is shown in Fig. 6.

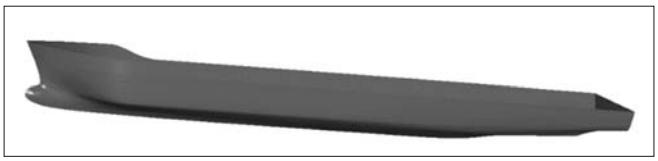

Fig. 6. The geometric model of the high-speed ship

Tab. 1. Main dimensions of high speed ship

Length between perpendiculars Lpp (m)	Breadth B(m)	Depth D(m)	Design draft d(m)	Displace-ment Δ(t)	Design speed (kn)
37.2	7.2	3.2	1.65	197	20

SHIP FORM OPTIMISATION

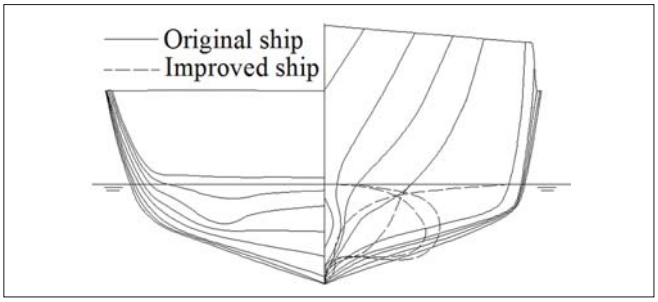

a) Bow optimisation

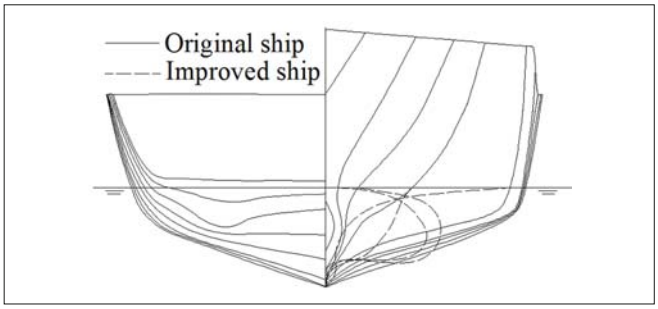

b) Full ship optimisation

Fig. 7. The comparison of body plans between the original hull form and the improved hull form (First optimisation)

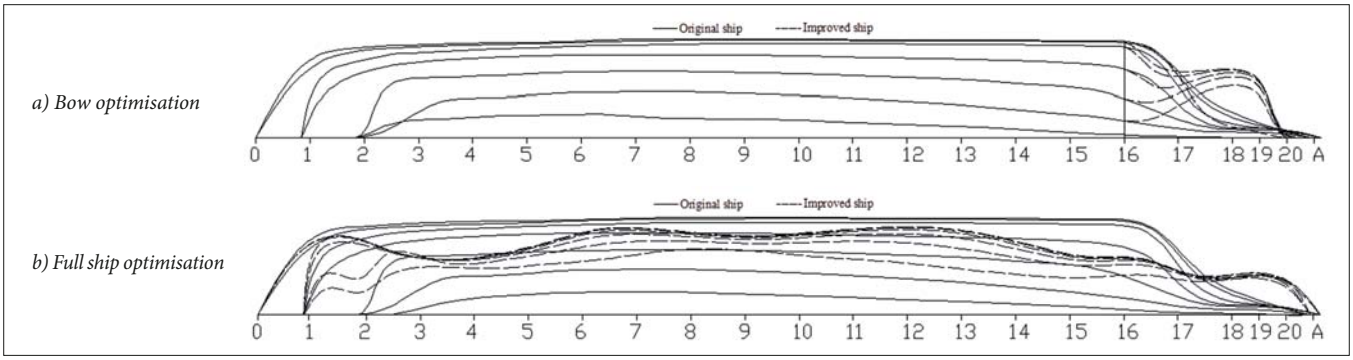

a) Bow optimisation

b) Full ship optimisation

Fig. 8. The comparison of waterlines between the original hull form and the improved hull form (First optimisation)

Tab. 2. Results of the first optimisation calculation

Ship hull	Con-straint	Speed	R_w/R_{w0}	R_F/R_{F0}	R_I/R_{T0}	V/V_0	S/S_0
Optimal ship1	1), 2)	20kn	42.4%	99.0%	61.2%	117.9%	99.0%
Optimal ship2	1), 2)	20kn	57.4%	91.8%	78.7%	100.0%	94.8%

Fig. 7 and Fig. 8 show the comparison of the cross-section and water line of the improved ship Type 1 obtained under the basic constraint conditions with those of the parent ship. The calculation results are summarised in Table 2. From the above calculation, it can be seen that although the drag reduction effect of the improved hull form is very obvious, the shape of the improved hull type is rather strange, and it is difficult to use in practice. Therefore, it needs additional constraints to re-optimise. However, such ship form is of great significance for guiding the ship form design and understanding the effect of the ship form change on resistance from a mechanism point of view.

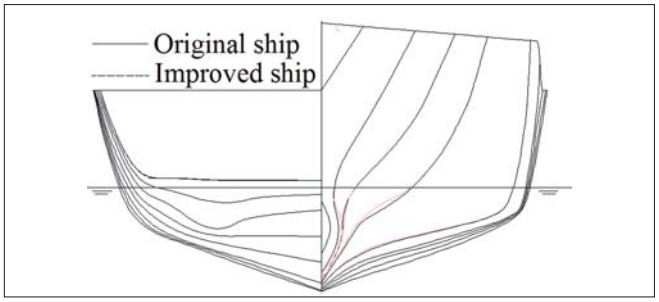

a) Bow optimisation

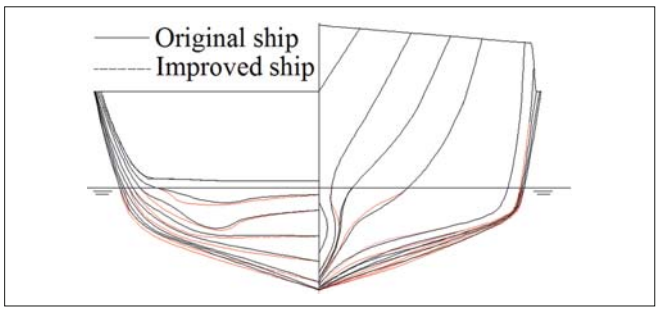

b) Full ship optimisation

Fig. 9. The comparison of body plans between the original hull form nd the improved hull form (Second optimisation)

Tab. 3. Results of the second optimisation calculation

Ship hull	Con-straint	Speed	R_w/R_{w0}	R_F/R_{F0}	R_I/R_{T0}	V/V_0	S/S_0
Optimal ship1	1),2),3)	20kn	88.4%	99.8%	94.2%	100.1%	99.6%
Optimal ship2	1),2),3)	20kn	83.6%	100.3%	90.7%	100.5%	100.2%

Because the ship form obtained by the first optimisation is strange and lacks practical significance, the additional constraint condition 3) is added and an improved ship form is obtained by re-optimisation. The comparison of the cross-section line and waterline with the parent ship form is shown in Fig. 9 and Fig. 10. The results of the optimisation calculation are summarised in Table 3. From the above calculation results, it can be seen that although the change in the line shape of the improved ship type is not as big as that of the first optimised hull, it also achieves an obvious resistance reduction effect, and its shape is closer to that of the practical ship type.

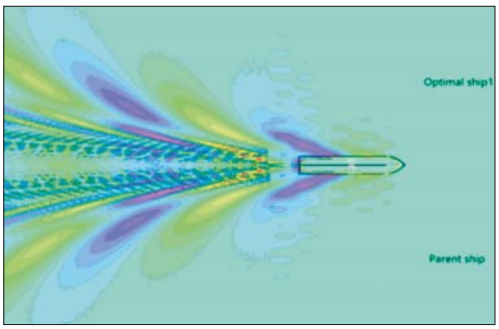

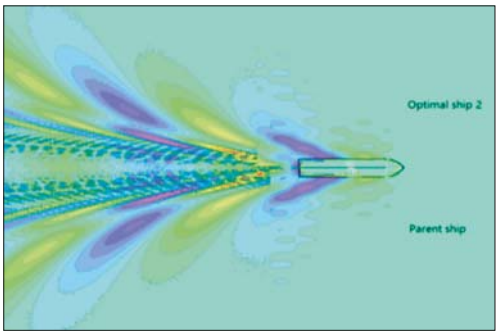

Fig. 11. Comparison of waveforms between optimised ship form and parent ship form

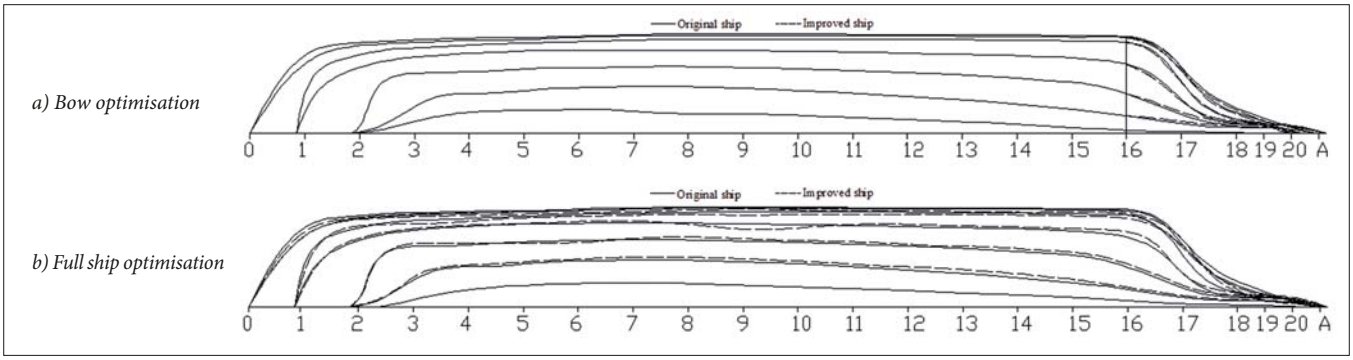

Fig. 10. The comparison of waterlines between the original hull form and the improved hull form (Second optimisation)

From Fig. 11, it can be seen that both the bow optimisation (Optimal ship one) and the whole ship optimisation (Optimal ship two) have an obvious drag reduction effect, but the free surface waveforms of the optimal ship form obtained by the two schemes are not much different from that of the parent ship type, which indicates that, with the prediction method of ship resistance based on potential flow theory, it is difficult to reflect the effect of small changes in ship form on the drag performance.

EVALUATION OF VISCOUS FLOW THEORY

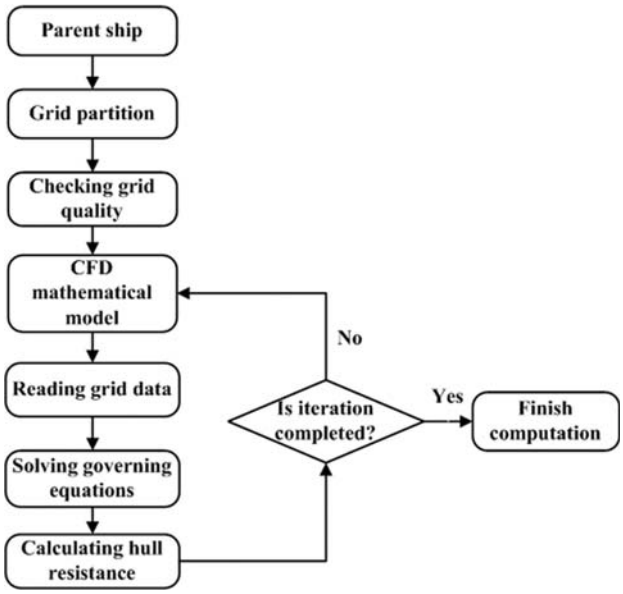

Fig. 12. Prediction process of resistance

The accuracy of using CFD to predict ship resistance has been accepted by engineering circles. Therefore, the CFD method is used to verify the final drag reduction effect of the improved ship type. Firstly, the geometric model is established, the mesh is divided, the mesh quality is checked, and the appropriate boundary conditions are set. A three-dimensional unsteady separation implicit solver is used; the continuous equation and N-S equation are used as the governing equations of the whole model, and the RNG k-ε turbulence model is chosen to solve the whole flow field; the free surface is captured by the VOF method; the pressure field and velocity field are coupled by the Pressure-Implicit with Splitting of Operators (PISO) method; taking the speed equal to the speed of the vehicle as the initial speed of the calculation, the iteration is calculated. The detailed calculation process is shown in Fig. 12.

COMPUTING DOMAIN AND BOUNDARY CONDITIONS

CFD software is used to build a three-dimensional numerical wave tank. Considering the parameters of wavelength, period and wave height of the simulated linear wave, the flume with a primary calculation domain scale of $4.5L \times 2.0L \times 2.5L$ is selected as the research object. The inlet of the flume is L from the bow of the ship, and the water depth is $1.5L$. The specific size is shown in Fig. 13. The lower part is water, and the upper part is air.

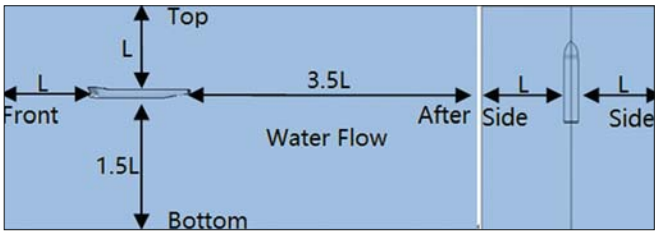

Fig. 13. Domain of simulation

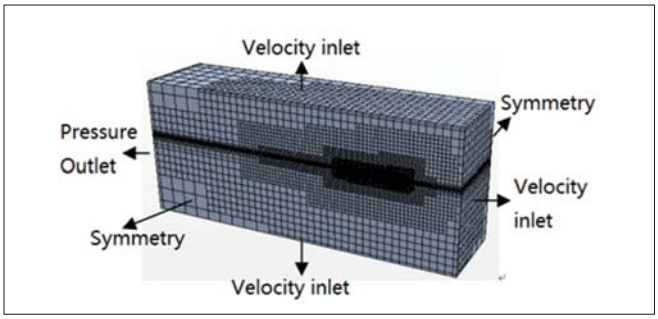

Fig. 14. Boundary conditions in domain

The front surface, upper surface and lower surface of the numerical simulation pool are set as the velocity inlet, and the inflow velocity, i.e. ship speed, is given at the front surface boundary; the back surface is set as the pressure outlet; the hull is set as a rigid wall; and the two sides are set as symmetrical as shown in Fig. 14.

GRID DIVISION AND QUALITY CHECK

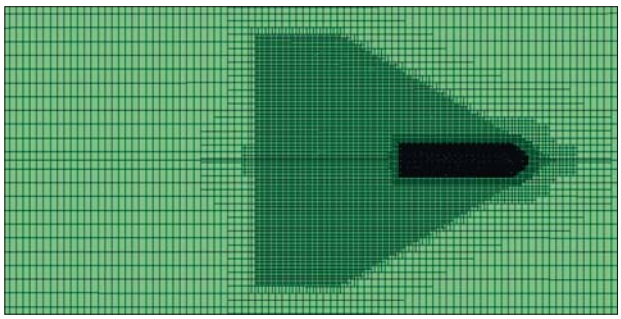

a) Seen from above onto the free surface

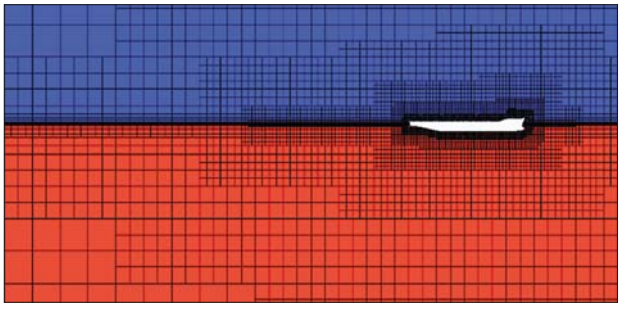

b) Seen from side to a plane midship

Fig. 15. Mesh scene on free surface

Mesh generation is an important part of numerical simulation. The quantity and quality of grids greatly affect the time and results of numerical simulation, and the quality of the grids plays a decisive role in the calculation accuracy. The area of the whole calculation is divided into a grid by the technology of a right-angle cutting grid. Considering the limitations of time and computer performance, a relatively sparse grid size is adopted for the basin, and only local mesh refinement is carried out at the fore and aft parts of the hull and at the free surface. The resulting number of grids is 1.38 million. Fig. 15 is the mesh generation of the free surface. From the graph, we can see that the grid near the ship's head and free surface is partially encrypted refined. Fig. 16 is the hull grid division.

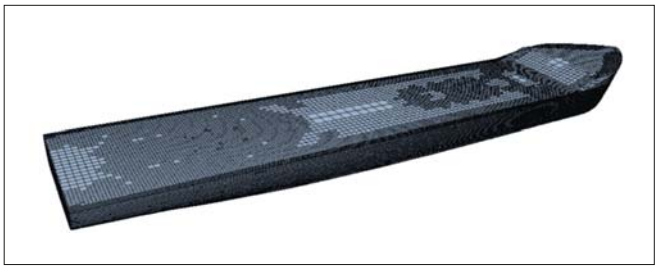

Fig. 16. Mesh scene on hull

The RANS flow solver embedded into STAR-CCM+ is used for all simulations using the free-surface capturing approach (VOF method) and RNG k-ε turbulence model. To generate meshes for the dependency study, the initial cell sizes were multiplied with successive ratios of 1.25. The viscous layer area is meshed to be compatible with a wall function (first cell size made to ensure a y+ around 30, expansion ratio of 1.2). The different numbers of cells are given in Table 4. For a speed of 20 kn, the results for the total resistance RT are given. With the increase of the number of grids, the total resistance does not change much. All the research in this paper is based on a medium number of grids of 1.38 million.

THE EVALUATION OF THE RESISTANCE REDUCTION

The effect of drag reduction evaluated by the CFD method is summarised in Table 5. It can be seen from the table that the drag reduction effect of the improved ship form is very obvious, whether the bow or the whole ship is optimised. The pressure resistance in the table can be considered as wave resistance, because the ship is a high-speed ship, and the shear resistance is mainly friction resistance. Although the pressure resistance has decreased greatly, the total resistance has not been reduced much. The main reason is that in addition to the increase of shear resistance, other resistance components may also increase, such as splash resistance. Therefore, when optimising the ship form with a certain resistance component as the main target, we must pay attention to the fact that other resistance components cannot be increased too much, so as to achieve the ultimate drag reduction effect.

Tab. 5. CFD method for evaluating optimisation results

Ship hull	R_W/R_{W0}	R_F/R_{F0}	R_T/R_{T0}
Optimal ship 1	86.6%	102.3%	92.6%
Optimal ship 2	83.4%	105.6%	95.3%

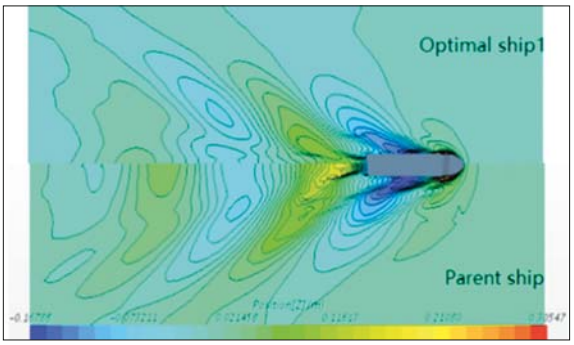

a) Full ship optimisation

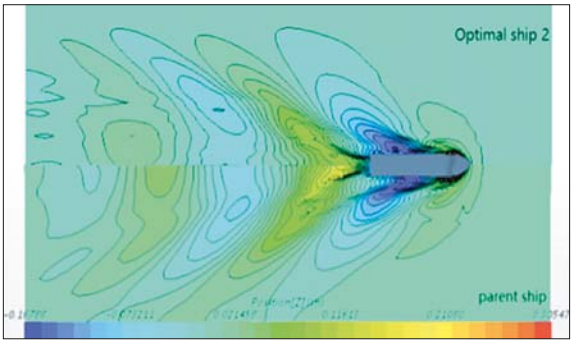

b) Bow optimisation
Fig. 17. Waveform diagram of free surface

Fig. 17 is a waveform comparison of two optimised ship types. As can be seen from the figure, the waveform of the optimal hull form obtained by the two optimisation schemes has changed considerably compared with the parent ship. However, the calculation method based on potential

Tab. 4. Number of cells for the mesh dependency study

Mesh schemes	Case1	Case2	*Case3*	*Case4*	*Case5*	*Case6*	*Case7*
Mesh density (millions)	0.31M	0.68M	0.84M	1.38M	2.0M	2.43M	4.35M
Total resistance coefficient $\times 10^3$	3.16	3.15	3.14	3.15	3.10	3.15	3.17

flow theory cannot reflect this change. This is the advantage of the CFD method, which can capture the influence of small changes of ship form on the flow field. When the bow optimisation is carried out, the bow wave of the optimal ship one system becomes narrower, and the wave system at other positions does not change much. When the whole ship is optimised, the whole wave system of the optimal ship two changes; especially the tail changes greatly, and the angle of the wave system becomes larger, so other resistance may increase.

CONCLUSION

(1) Taking the total resistance as the objective function (in which the wave-making resistance is calculated by the Michell integral and the viscous resistance is expressed by the function of the wet surface area), the hull surface value as the design variable and no reduction in drainage capacity as the basic constraints, then considering the additional constraints of practical ship form, a mathematical model of a non-linear programming method is established for carrying out optimisation research of a bow or full ship shape.
(2) Taking the real ship (wind power operation and maintenance vessel) as the initial ship type, at a given design speed, the bow and the whole ship shape are optimised by adding different constraints. Two improved ship types are obtained. Compared with the original ship type, the wave-making resistance of the more practical improved ship type obtained by the second optimisation is reduced by 11.6% and 16.4% respectively, and the total resistance is reduced by 5.8% and 9.3% respectively.
(3) The results show that the wave-making resistance of the two improved hulls decreases by 13.4% and 16.6%, respectively, and the total resistance decreases by 7.4% and 4.7%, respectively. From the calculation results, it can be seen that both improved hulls have obvious drag-reducing effects.
(4) For a real ship, the calculation of wave-making resistance by the CFD method is closer to the experimental value than that by the Michell integral. If the CFD method is used instead of the Michell integral and added to the objective function for optimisation calculation, the improved ship form will be better optimised and more reliable, which is the next step of this study.

ACKNOWLEDGEMENTS

Foundation item: The National Natural Science Foundation of China (No: 51009087, No: 51779135); Shanghai Natural Science Fund Project (No: 14ZR1419500); Numerical simulation of the propagation of internal solitary waves in South China Sea (No: 17040501600).

REFERENCES

1. Kim H. J., Choi J. E., Chun H. H. (2016): *Hull-form optimization using parametric modification functions and particle swarm optimization*. Journal of Marine Science and Technology, 21, 129–144.
2. Li G. L., Long L. H., Tan Z. S. (1990): *Energy-saving ship design*. National Defense Industry press, Beijing, China.
3. Liu X. Y., Wu J. W., Wan D. C. (2016): *Ship type optimization based on genetic algorithm and NM theory.* Hydrodynamic Research and Development, 31(5), 535–541.
4. Li Z. Z. (2005): *Research on ship type optimization based on wave resistance value calculation*. Dalian University of Technology, China.
5. Luo W. L., Lan L. Q. (2017): *Design Optimization of the Lines of the Bulbous Bow of a Hull Based on Parametric Modeling and Computational Fluid Dynamics Calculation*. Math Computation. Appl., 22(1), 43–54.
6. Masut S., Suzuki K. (2001): *Experimental Verification of Optimized Hull Form Based on Rankine Source Method*. J. Kansai Soc. N. A., Japan, 236, 27–32.
7. Ma K., Ichiro T. (1994): *A study of minimum resistance hull form with consideration of separation (1st Report)*. J. Kansai Soc. N. A., Japan, 221, 9–15.
8. Ma K., Zhang M. X., Ji Z. S. (2003): *Ship floating calculation based on nonlinear programming.* Journal of Dalian University of Technology, 43(3), 329–331.
9. Huang F. X., Wang L. J., Yang C. (2015): *Hull Form Optimization for Reduced Drag and Improved Seakeeping Using a Surrogate-Based Method.* 25th International Ocean and Polar Engineering Conference, Kona, Big Island, Hawaii, USA.
10. Hirt C. W., Nichols B. D. (1981): *Volume of fluid (VOF) method for the dynamics of free boundaries.* Journal of Computational Physics, 39(1), 201–225.
11. Hsiung C. C. (1981): *Optimal Ship Forms for Minimum Wave Resistance.* Journal of Ship Research, 25(2), 95–116.
12. Hsiung C. C. (1984): *Optimal Ship Forms for Minimum Total Resistance*. Journal of Ship Research, 28(3), 163–172.
13. Wang S., Chen J. P., Wei J. F. (2013): *The development and application research of an integrated optimization system based on the resistance in calm water and added resistance due to waves.* 25th National Hydrodynamics Seminar and 12th National Hydrodynamics Academic Conference, Zhejiang, Zhoushan, 928–933.

14. Wu J. W., Liu X. Y. and Wan D. C. (2016): *Multi-Objective Hydrodynamic Optimization of Ship Hull Based on Approximation Model*. Proceedings of 26th (2016) International Ocean and Polar Engineering Conference Rhodes, Greece.

15. Ye H. K. (1985): *The wave resistance calculation and optimization of ship form with the tent function.* Shipbuilding of China, 1985, 28–39.

16. Zhang W. X. (2012): *Comprehensive optimization of hull form for containership in wave based on EEDI*. Wuhan University of Technology, China, Wuhan.

17. Zhang S. L., Zhang B. J., Tezdogan T. et al. (2017): *Computational fluid dynamics based hull form optimization using approximation method.* Engineering Applications of Computational Fluid Mechanics, 12(3), 1–8.

18. Zhang S. L., Zhang B. J., Tezdogan T. et al. (2017): *Research on bulbous bow optimization based on the improved PSO algorithm.* China Ocean Engineering, 33(4), 487–494.

19. Zhang S. L., Tezdogan T., Zhang B. J. et al. (2017): *Hull form optimization in waves based on CFD technique.* Ships & Offshore Structures, 12(2), 1–16.

20. Zhang B. J., Zhang S. L. (2018): *Research on ship design and optimization based on simulation-based design (SBD) Technique*. Shanghai Jiaotong University Press and Springer.

21. Zou Y. (2012): *Research on optimization method for high performance vessel Research on optimization method for high performance vessel.* Dalian Maritime University, China, Dalian.

CONTACT WITH The AUTHORS

Zhang Baoji
e-mail: zbj1979@163.com

Shanghai Maritime University
1550 Haigang Av, 201306 Shanghai
China